JCEC
THE JOURNAL OF ENGINEERING AND EXACT SCIENCES

OPEN ACCESS

The Journal of Engineering and Exact Sciences – jCEC, Vol. 08 N. 08 (2022)
journal homepage: https://periodicos.ufv.br/jcec
eISSN: 2527-1075
ISSN: 2446-9416

Comparative Analysis of Temperature Distributions in a Convective-Radiative Porous Fin using Homotopy Perturbation and Differential Transformation and Methods

Article Info:
Article history: Received 2022-09-09 / Accepted 2022-11-01 / Available online 2022-11-01
doi: 10.18540/jcecvl8iss8pp14924-01i

Gbeminiyi Musibau Sobamowo
ORCID: https://orcid.org/0000-0003-2402-1423
Department of Mechanical Engineering, Faculty of Engineering, University of Lagos, Akoka Lagos, Nigeria
E-mail: gsobamowo@unilag.edu.ng
Suraju Aremu Oladosu
Department of Mechanical Engineering, Faculty of Engineering, Lagos State University, Epe Campus, Lagos, Nigeria
E-mail: suraju.oladosu@lasu.edu.ng
Rafiu Olalekan Kuku
Department of Mechanical Engineering, Faculty of Engineering, Lagos State University, Epe Campus, Lagos, Nigeria
E-mail: rafiu.kuku@lasu.edu.ng
Antonio Marcos de Oliveira Siqueira
ORCID: https://orcid.org/0000-0001-9334-0394
Federal University of Viçosa, Brazil
E-mail: antonio.siqueira@ufv.br

Abstract
In this work, a comparative study of two approximate analytical methods for the thermal behaviour of convective-radiative porous fin subjected to the magnetic field using homotopy perturbation and differential transform methods is presented. Also, parametric studies of the effects of thermal-geometric and thermo-physical fin parameters are investigated. From the study, it is found that an increase in a magnetic field, porosity, convective, radiative, and parameters increase the rate of heat transfer from the fin and consequently improves the efficiency of the fin. There are good agreements between the results of the homotopy perturbation and differential transform method with the results of the numerical method. Also, the results of the two approximate analytical methods agree very well with each other. It is hoped that the present work will serve as the basis of verifications of the other works on the nonlinear thermal analysis of the extended surface.
Keywords: Comparative method study; Thermal analysis; Porous Fin; Convective-Radiative fin; Magnetic field; Homotopy perturbation method; Differential transformation method

Nomenclature

a_r aspect ratio ratio of the porous fin base area to the surface area
A cross sectional area of the fins, m^2
A_b porous fin base area
A_s porous fin surface area
Bi Biot number
h heat transfer coefficient, $Wm^{-2}k^{-1}$
h_b heat transfer coefficient at the base of the fin, $Wm^{-2}k^{-1}$
c_p specific heat of the fluid passing through porous fin(J/kg-K)
Da Darcy number
g gravity constant(m/s^2)
h heat transfer coefficient over the fin surface (W/m^2K)
H dimensionless heat transfer coefficient at the base of the fin, $Wm^{-2}k^{-1}$
k thermal conductivity of the fin material, $Wm^{-1}k^{-1}$
k_b thermal conductivity of the fin material at the base of the fin, $Wm^{-1}k^{-1}$
k_{eff} effective thermal conductivity ratio
K permeability of the porous fin (m^2)
L Length of the fin, m
M dimensionless thermo-geometric parameter
m mass flow rate of fluid passing through porous fin(kg/s)
Nu Nusselt number
P perimeter of the fin(m)
Q dimensionless heat transfer rate per unit area
q_b heat transfer rate per unit area at the base (W/m^2)
Q_b dimensionless heat transfer rate the base in porous fin
Q_s dimensionless heat transfer rate the base in solid fin
Ra Rayleigh number
S_h Porosity parameter
t thickness of the fin
T_b base temperature(K)
T fin temperature (K)
T_a ambient temperature, K
T_b Temperature at the base of the fin, K
v average velocity of fluid passing through porous fin(m/s)
x axial length measured from fin tip (m)
X dimensionless length of the fin
w width of the fin
q internal heat generation in W/m^3

Greek Symbols

β thermal conductivity parameter or non-linear parameter
δ thickness of the fin, m
δ_b fin thickness at its base.
γ dimensionless internal heat generation parameter
θ dimensionless temperature
θ_b dimensionless temperature at the base of the fin
η efficiency of the fin
ε effectiveness of the fin
β' coefficient of thermal expansion(K^{-1})
ε porosity or void ratio
υ kinematic viscosity(m^2/s)
ρ density of the fluid(kg/m^3)

Subscripts

s solid properties
f fluid properties
eff effective porous properties

1. Introduction

The continuous demands and production of high-performance equipment have parts of the driving forces behind the present advancement in technology. However, in many of such equipment, excess heat generation is unavoidable. Therefore, the removal of the excess heat by effective cooling technology is very vital for reliable operation, proper functioning and performance of the equipment. In removing the heat, it is obvious the use of fins or extended surface plays an essential and a very important role among various passive and active cooling options. Also, in the search of enhancing and augmenting the rate of heat transfer by fins from the prime surfaces, it has been found that the use of porous fin with certain porosity may give same performance as convectional fin and save 100ϕ of the fin material (Kiwan & Al-Nimr, 2014).

The discovery of this idea has led to numerous studies and extensive research on the use of porous fins. The pioneer work on the heat transfer enhancement through the use of porous was carried out by Kiwan & Al-Nimr (2014). They applied numerical method to investigate the thermal analysis of porous fin while Kiwan (2007a and 2007b), and Kiwan & Zeitoun (2008) developed a simple method to study the performance of porous fins in natural convection environment. Also, the same authors investigated the effects of radiative losses on the heat transfer from porous fins.

Gorla and Bakier (2007) numerically carried out the thermal analysis of natural convection and radiation in a rectangular porous fin. Kundu & Bhanja (2011) presented analytical model for the analysis of performance and optimization of porous fins. Kundu *et al.* (2012) proposed a model for computing maximum heat transfer in porous fins. Taklifi *et al.* (2010) investigated the effects of magnetohydrodynamics (MHD) on the performance of a rectangular porous fin. In the work, that by imposing MHD in system except near the fin tip, heat transfer rate from the porous fin decreases. Bhanja & Kundu (2011) analytically investigated thermal analysis of a constructal T-shape porous fin with radiation effects. An increase in heat transfer is found by choosing porous medium condition in the fin.

Kundu *et al.* (2007) applied Adomian decomposition method on the performance and optimum design analysis of porous fin of various profiles operating in convection environment transient heat transfer analysis of variable section pin fins. Saedodin and Sadeghi (2013) analyzed the heat transfer in a cylindrical porous fin while Saedodin & Olank (2011). Darvishi *et al.* (2015) studied the thermal performance of a porous radial fin with natural convection and radiative heat losses while Hatami and Ganji (2013) investigated the thermal performance of circular convective-radiative porous fins with different section shapes and materials. Hatami *et al. (2013),* Hatami & Ganji (2014a, 2014b), Hatami *et al.* (2014) presented various heat transfer studies in both dry and wet porous fins.

In solving the heat transfer problem in porous fin, Kundu (2007), Kundu & Bhanji (2011), and Kundu *et al.* (2012) applied Adomian decomposition method (ADM) on the performance and optimum design analysis of the fins while Gorla & Bakier (2007), Kiwan (2007a and 2007b), Kiwan & Zeitoun (2008), Saedodin & Sadeghi (2013), and Kiwan & Al-Nimr (2014) applied Runge-Kutta for the thermal analysis in porous fin.

Golar and Baker (2007) and Gorla *et al*. (2013) applied Spectral collocation method (SCM) to study the effects of variable thermal conductivity on the natural convection and radiation in porous fin. Saedodin and Shahababaei (2013) adopted Homotopoy perturbation method (HPM) to analyse heat transfer in longitudinal porous fins while Darvishi *et al.* (2015), Moradi *et al.* (2014) and Hoshyar, Ganji, and Abbasi (2015) adopted Homotopy analysis method (HAM) to provide solution to the natural convection and radiation in a porous and porous moving fins while Hoshyar *et al.* (2015) used Homotopy perturbation method and collocation method for Thermal performance analysis of porous fins with temperature-dependent heat generation.

Hatami and Ganji (2013) applied least square method (LSM) to study the thermal behaviour of convective-radiative in porous fin with different sections and ceramic materials. Also, Rostamiyan *et al*. (2014) applied variational iterative method (VIM) to provide analytical solution for heat transfer in porous fin. Ghasemi *et al.* (2014) used differential transformation method (DTM) for heat transfer analysis in porous and solid fin while Petroudi *et al.* (2012) utilized both HPM and HAM to solve nonlinear equation arising in a natural convection porous fin. Amirkolaei *et al.* (2014) applied homotopy analysis method and collocation method while Hoshyar et al. (2016) used least square method to predict the temperature distribution in a porous fin which is exposed to uniform magnetic field. In this work, comparative study of two approximate analytical methods for thermal behaviour of convective-radiative porous fin subjected to magnetic field using homotopy perturbation and differential transformation methods is presented. Parametric studies of the effects of thermal-geometric and thermo-physical fin parameters are investigated. The developed symbolic thermal solutions are used to investigate the effects of convective, radiative, magnetic parameters on the thermal performance of the porous fin.

2. Problem formulation

Consider a convective-radiative porous fin of length L and thickness *t* exposed on both faces to a convective environment at temperature T_∞ and subjected to magnetic field as shown in Figure 1. The dimension *x* pertains to the height coordinate which has its origin at the fin tip and has a positive orientation from fin tip to fin base. In order to analyze the problem, the following assumptions are made.

1. Porous medium is homogeneous, isotropic and saturated with a single-phase fluid
2. Physical properties of solid as well as fluid are considered as constant except density variation of liquid, which may affect the buoyancy term where Boussinesq approximation is employed.
3. Fluid and porous mediums are locally thermodynamic equilibrium in the domain.
4. Surface convection, radiative transfers and non-Darcian effects are negligible.
5. The temperature variation inside the fin is one-dimensional i.e., temperature varies along the length only and remain constant with time.
6. There is no thermal contact resistance at the fin base and the fin tip is adiabatic type.

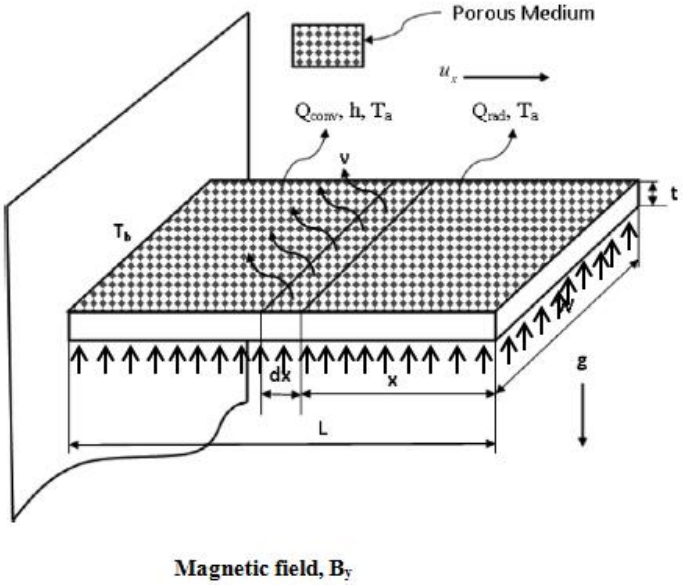

Figure 1 Schematic of the convective-radiative longitudinal porous fin with magnetic field fin

Based on Darcy's model and following the above assumptions, the thermal energy balance could be expressed

$$q_x - \left(q_x + \frac{\delta q}{\delta x} dx \right) + q(T)\,dx = \dot{m} c_p (T - T_a) + hP(T - T_a)dx + \sigma \varepsilon P(T^4 - T_a^4)dx + \frac{J_c \times J_c}{\sigma} dx \quad (1)$$

where

$$J_c = \sigma \left(E + V \times B \right) \quad (2)$$

The mass flow rate of the fluid passing through the porous material can be written as

$$\dot{m} = \rho u(x) W dx \quad (3)$$

From the Darcy's Model

$$u(x) = \frac{gK\beta}{\nu} \left(T - T_a \right) \quad (4)$$

Therefore, Equation (1) becomes

$$q_x - \left(q_x + \frac{\delta q}{\delta x} dx \right) = \frac{\rho c_p g K \beta}{\nu} (T - T_a)^2 dx + hP(T - T_a)dx + \sigma \varepsilon P(T^4 - T_a^4)dx + \frac{J_c \times J_c}{\sigma} dx \quad (5)$$

As $dx \rightarrow 0$, Equation (5) reduces

$$-\frac{dq}{dx} = \frac{\rho c_p g K \beta}{\nu} (T - T_a)^2 + hP(T - T_a) + \sigma \varepsilon P(T^4 - T_a^4)dx + \frac{J_c \times J_c}{\sigma} \quad (6)$$

From Fourier's law of heat conduction, the rate of heat conduction in the fin is given by

$$q = -k_{eff} A_{cr} \frac{dT}{dx} \quad (7)$$

where

$$k_{eff} = \phi k_f + (1 - \phi) k_s$$

Following Rosseland diffusion approximation, the radiation heat transfer rate is

$$q = -\frac{4\sigma A_{cr}}{3\beta_R} \frac{dT^4}{dx} \quad (8)$$

Therefore, the total rate of heat transfer is given by

$$q = -k_{eff} A_{cr} \frac{dT}{dx} - \frac{4\sigma A_{cr}}{3\beta_R} \frac{dT^4}{dx} \quad (9)$$

Substituting Equation (9) into Equation (6), we have

$$\frac{d}{dx} \left(k_{eff} A_{cr} \frac{dT}{dx} + \frac{4\sigma A_{cr}}{3\beta_R} \frac{dT^4}{dx} \right) = \frac{\rho c_p g K \beta}{\nu} (T - T_a)^2 + hP(T - T_a) + \sigma \varepsilon P(T^4 - T_a^4)dx + \frac{J_c \times J_c}{\sigma} \quad (10)$$

Further simplification of Equation (10) gives the governing differential equation for the fin as

$$\frac{d^2T}{dx^2}+\frac{4\sigma}{3\beta_R k_{eff}}\frac{d}{dx}\left(\frac{dT^4}{dx}\right)-\frac{\rho c_p gK\beta}{k_{eff}tv}(T-T_a)^2-\frac{h}{k_{eff}t}(T-T_a)-\frac{\sigma\varepsilon}{k_{eff}t}(T^4-T_a^4)dx-\frac{J_c\times J_c}{\sigma k_{eff}A_{cr}}=0 \quad (11)$$

The boundary conditions are

$$\begin{aligned} &x=0, \quad \frac{dT}{dx}=0 \\ &x=L, \quad T=T_b \end{aligned} \quad (12)$$

But

$$\frac{J_c\times J_c}{\sigma}=\sigma B_o^2u^2 \quad (13)$$

After substitution of Equation (13) into Equation (11), taking the magnetic term as a linear function of temperature, we have

$$\frac{d^2T}{dx^2}+\frac{4\sigma}{3\beta_R k_{eff}}\frac{d}{dx}\left(\frac{dT^4}{dx}\right)-\frac{\rho c_p gK\beta}{k_{eff}tv}(T-T_a)^2-\frac{h}{k_{eff}t}(T-T_a)-\sigma\varepsilon P(T^4-T_a^4)dx-\frac{\sigma B_o^2u^2}{k_{eff}A_{cr}}(T-T_a)=0 \quad (14)$$

The case considered in this work is a situation where small temperature difference exists within the material during the heat flow. This actually necessitated the use of temperature-invariant physical and thermal properties of the fin. Also, it has been established that under such scenario, the term T^4 can be expressed as a linear function of temperature. Therefore, we have

$$T^4=T_\infty^4+4T_\infty^3\left(T-T_\infty\right)+6T_\infty^2\left(T-T_\infty\right)^2+\ldots\cong 4T_\infty^3T-3T_\infty^4 \quad (15)$$

On substituting Equation (15) into Equation (14), we arrived at

$$\frac{d^2T}{dx^2}+\frac{16\sigma}{3\beta_R k_{eff}}\frac{d^2T}{dx^2}-\frac{\rho c_p gK\beta}{k_{eff}tv}(T-T_a)^2-\frac{h}{k_{eff}t}(T-T_a)-4\sigma\varepsilon PT_a^3(T-T_a)dx-\frac{\sigma B_o^2u^2}{k_{eff}A_{cr}}(T-T_a)=0 \quad (16)$$

On introducing the following dimensionless parameters in Equation (17) into Equation (16),

$$X=\frac{x}{L},\ \theta=\frac{T-T_a}{T_b-T_a} \quad Ra=\frac{gk\beta\left(T_b-T_\infty\right)b}{\alpha\nu k_r} \quad Nc=\frac{pbh}{A_b k_{eff}} \quad Rd=\frac{4\sigma_{st}T_\infty^3}{3\beta_R k_{eff}} \quad Nr=\frac{4\sigma_{st}bT_\infty^3}{k_{eff}} \quad H=\frac{\sigma B_0^2u^2}{k_{eff}A_b}. \quad (17)$$

we arrived at the dimensionless form of the governing Equation (16) as

$$\left(1+4Rd\right)\frac{d^2\theta}{dX^2}-Ra\theta^2-Nc(1-\varepsilon)\theta-Nr\theta-H\theta=0 \quad (18)$$

and the dimensionless boundary conditions

$$X = 0, \quad \frac{d\theta}{dX} = 0$$
$$X = 1, \quad \theta = 1 \tag{19}$$

3. Method of Solution: Differential Transform Method

It is very difficult to develop a closed-form solution for the above non-linear equation (18). Therefore, recourse has to be made to either approximation analytical method, semi-numerical method or numerical method of solution. In this work, differential transform method is used. The basic definitions of the method is as follows

If $u(t)$ is analytic in the domain T, then it will be differentiated continuously with respect to time *t.*

$$\frac{d^p u(t)}{dt^p} = \varphi(t, p) \qquad \text{for} \qquad \text{all } t \in T \tag{20}$$

for $t = t_i$, then $\varphi(t, p) = \varphi(t_i, p)$, where *p* belongs to the set of non-negative integers, denoted as the *p*-domain. Therefore Equation (50) can be rewritten as

$$U(p) = \varphi(t_i, p) = \left[\frac{d^p u(t)}{dt^p} \right]_{t=t_i} \tag{21}$$

Where U_p is called the spectrum of $u(t)$ at $t = t_i$

If $u(t)$ can be expressed by Taylor's series, the $u(t)$ can be represented as

$$u(t) = \sum_{p}^{\infty} \left[\frac{(t - t_i)^p}{p!} \right] U(p) \tag{22}$$

Where Equ. (22) is called the inverse of $U(k)$ using the symbol 'D' denoting the differential transformation process and combining (21) and (22), it is obtained that

$$u(t) = \sum_{p=0}^{\infty} \left[\frac{(t - t_i)^p}{p!} \right] U(p) = D^{-1} U(p) \tag{23}$$

3.1 Operational properties of differential transformation method

If $u(t)$ *and* $v(t)$ are two independent functions with time (t) where $U(p)$ and $V(p)$ are the transformed function corresponding to $u(t)$ and $v(t)$, then it can be proved from the fundamental mathematics operations performed by differential transformation that.

i. If $z(t)=u(t)\pm v(t)$, then $Z(p)=U(p)\pm V(p)$

ii. If $z(t)=\alpha u(t)$, then $Z(p)=\alpha U(p)$

iii. If $z(t)=\dfrac{du(t)}{dt}$, then $Z(p)=(p-1)\,U(p+1)$

iv. If $z(t)=u(t)v(t)$, then $Z(t)=\sum_{r=0}^{p}V(r)U(p-r)$

v. If $z(t)=u^{m}(t)$, then $Z(t)=\sum_{r=0}^{p}U^{m-1}(r)U(p-r)$

vi. If $z(t)=u(t)v(t)$, then $Z(k)=\sum_{r=0}^{p}(r+1)V(r+1)U(p-r)$

The differential transformation of the governing differential Equation (18) is given as

$$\left(1+4Rd\right)(k+1)(k+2)\theta(k+2)-Ra\sum_{l=0}^{k}\begin{bmatrix}\theta(l)\theta(k-l)-Nc(1-\varepsilon)\theta(k)\\-Nr\theta(k)-H\theta(k)\end{bmatrix}=0 \tag{24}$$

and the boundary condition in Equation (19)

$k=0,\quad \theta(1)=0$

$\sum_{l=0}^{k}\theta(1)=1 \quad\Rightarrow\quad \theta(0)=a$

Equation (24) could be further simplified as

$$\theta(k+2)=\frac{Ra}{\left(1+4Rd\right)(k+1)(k+2)}\left\{\sum_{l=0}^{k}\begin{bmatrix}\theta(l)\theta(k-l)+Nc(1-\varepsilon)\theta(k)\\+Nr\theta(k)+H\theta(k)\end{bmatrix}\right\} \tag{25}$$

Which can be written as

$$\theta(k+2)=\frac{\alpha_1}{(k+1)(k+2)}\sum_{l=0}^{k}\left[\theta(l)\theta(k-l)\right]+\frac{\alpha_2}{(k+1)(k+2)}\theta(k) \tag{26}$$

where

$$\alpha_1=\frac{Ra}{\left(1+4Rd\right)},\quad \alpha_2=\frac{Nc(1-\varepsilon)+Nr+H}{\left(1+4Rd\right)}$$

Now for the counter k=0, 1, 2, 3,..., N in Equation (26), we have

$\theta(0)=a$

$\theta(1)=0$

$$\theta(2)=\frac{1}{2}\left(a^2\alpha_1+a\alpha_2\right)$$

$$\theta(3)=0$$

$$\theta(4)=\frac{1}{24}\left(2a^3\alpha_1^2+3a^2\alpha_1\alpha_2+\alpha_1\alpha_2^2\right)$$

$$\theta(5)=0$$

$$\theta(6)=\frac{1}{720}\left(10a^4\alpha_1^3+20a^3\alpha_1^2\alpha_2+11a^2\alpha_1\alpha_2^2+a\alpha_2^3\right)$$

$$\theta(7)=0$$

$$\theta(8)=\frac{1}{40320}\left(80a^5\alpha_1^4+200a^4\alpha_1^3\alpha_2+162a^3\alpha_1^3\alpha_2^2+43a^2\alpha_1\alpha_2^3+a\alpha_2^4\right)$$

$$\theta(9)=0$$

$$\theta(10)=\frac{1}{3628800}\left(\begin{array}{l}1000a^6\alpha_1^5+3000a^5\alpha_1^4\alpha_2+3170a^4\alpha_1^3\alpha_2^2+1340a^3\alpha_1^2\alpha_2^3\\+171a^2\alpha_1\alpha_2^4+a\alpha_2^5\end{array}\right)$$

$$\theta(11)=0$$

$$\theta(12)=\frac{1}{476001600}\left(\begin{array}{l}17600a^7\alpha_1^6+61600a^6\alpha_1^5\alpha_2+80560a^5\alpha_1^4\alpha_2^2+\\47400a^4\alpha_1^3\alpha_2^3+11522a^3\alpha_1^2\alpha_2^4+683a^2\alpha_1\alpha_2^5+a\alpha_2^6\end{array}\right)$$

$$\theta(13)=0$$

$$\theta(14)=\frac{1}{87178291200}\left(\begin{array}{l}418000a^8\alpha_1^7+1672000a^7\alpha_1^6\alpha_2+2604000a^6\alpha_1^5\alpha_2^2+\\1960000a^5\alpha_1^4\alpha_2^3+7087300a^4\alpha_1^3\alpha_2^4+101460a^3\alpha_1^2\alpha_2^5+\\2731a^2\alpha_1\alpha_2^6+a\alpha_2^7\end{array}\right)$$

$$\theta(15)=0$$

$$\theta(16)=\frac{1}{20922789888000}\left(\begin{array}{l}12848000a^9\alpha_1^8+57816000a^8\alpha_1^7\alpha_2+104504800a^7\alpha_1^6\alpha_2^2\\+95958800a^6\alpha_1^5\alpha_2^3+46309440a^5\alpha_1^4\alpha_2^4+10780600a^4\alpha_1^3\alpha_2^5\\+904082a^3\alpha^2{}_1\alpha_2^6+10923a^2\alpha_1\alpha_2^7+a\alpha_2^8\end{array}\right)$$

$$\theta(17)=0$$

$$\theta(18)=\frac{1}{642373705728000}\begin{pmatrix}496672000a^{10}\alpha_1^9+248336000a^9\alpha_1^8\alpha_2+5109512000a^8\alpha_1^7\alpha_2^2\\+5537888000a^7\alpha_1^6\alpha_2^3+3348125000a^6\alpha_1^5\alpha_2^4+1091879000a^5\alpha_1^4\alpha_2^5\\+166874690a^4\alpha_1^3\alpha_2^6+8100380a^3\alpha_1^2\alpha_2^7+43691a^2\alpha_1\alpha_2^8+a\alpha_2^9\end{pmatrix}$$

From the definition of DTM, we have

$$\begin{aligned}\theta(X)=a+\frac{1}{2}\left(a^2\alpha_1+a\alpha_2\right)X^2+\frac{1}{24}\left(2a^3\alpha_1^2+3a^2\alpha_1\alpha_2+\alpha_1\alpha_2^2\right)X^4+\frac{1}{720}\left(10a^4\alpha_1^3+20a^3\alpha_1^2\alpha_2+11a^2\alpha_1\alpha_2^2+a\alpha_2^3\right)X^6+\\ \frac{1}{40320}\left(80a^5\alpha_1^4+200a^4\alpha_1^3\alpha_2+162a^3\alpha_1^2\alpha_2^2+43a^2\alpha_1\alpha_2^3+a\alpha_2^4\right)X^8+\\ \frac{1}{3628800}\left(1000a^6\alpha_1^5+3000a^5\alpha_1^4\alpha_2+3170a^4\alpha_1^3\alpha_2^2+1340a^3\alpha_1^2\alpha_2^3+171a^2\alpha_1\alpha_2^4+a\alpha_2^5\right)X^{10}+\\ \frac{1}{476001600}\begin{pmatrix}17600a^7\alpha_1^6+61600a^6\alpha_1^5\alpha_2+80560a^5\alpha_1^4\alpha_2^2+47400a^4\alpha_1^3\alpha_2^3+\\11522a^3\alpha_1^2\alpha_2^4+683a^2\alpha_1\alpha_2^5+a\alpha_2^6\end{pmatrix}X^{12}+\\ \frac{1}{87178291200}\begin{pmatrix}418000a^8\alpha_1^7+1672000a^7\alpha_1^6\alpha_2+2604000a^6\alpha_1^5\alpha_2^2+1960000a^5\alpha_1^4\alpha_2^3+\\+7087300a^4\alpha_1^3\alpha_2^4+101460a^3\alpha_1^2\alpha_2^5+2731a^2\alpha_1\alpha_2^6+a\alpha_2^7\end{pmatrix}X^{14}+\\ \frac{1}{20922789888000}\begin{pmatrix}12848000a^9\alpha_1^8+57816000a^8\alpha_1^7\alpha_2+104504800a^7\alpha_1^6\alpha_2^2+95958800a^6\alpha_1^5\alpha_2^3+\\46309440a^5\alpha_1^4\alpha_2^4+10780600a^4\alpha_1^3\alpha_2^5+904082a^3\alpha^2{}_1\alpha_2^6+10923a^2\alpha_1\alpha_2^7+a\alpha_2^8\end{pmatrix}X^{16}+\\ \frac{1}{642373705728000}\begin{pmatrix}496672000a^{10}\alpha_1^9+248336000a^9\alpha_1^8\alpha_2+5109512000a^8\alpha_1^7\alpha_2^2+5537888000a^7\alpha_1^6\alpha_2^3\\+3348125000a^6\alpha_1^5\alpha_2^4+1091879000a^5\alpha_1^4\alpha_2^5+166874690a^4\alpha_1^3\alpha_2^6+8100380a^3\alpha_1^2\alpha_2^7+\\43691a^2\alpha_1\alpha_2^8+a\alpha_2^9\end{pmatrix}X^{18}\end{aligned}$$

(27)

4. Method of Solution by homotopy Perturbation Method

It is very difficult to develop a closed-form solution for the above non-linear equation (19). Therefore, recourse has to be made to either approximation analytical method, semi-numerical method or numerical method of solution. In this work, homotopy perturbation method is used to solve the equation.

4.1 The basic idea of homotopy perturbation method

In order to establish the basic idea behind homotopy perturbation method, consider a system of nonlinear differential equations given as

$$A(U)-f(r)=0,\quad r\in\Omega \tag{28}$$

with the boundary conditions

$$B\left(u,\frac{\partial u}{\partial\eta}\right)=0,\qquad r\in\Gamma \tag{29}$$

where A is a general differential operator, B is a boundary operator, $f(r)$ a known analytical function and Γ is the boundary of the domain Ω

The operator *A* can be divided into two parts, which are *L* and *N*, where *L* is a linear operator, *N* is a non-linear operator. Equation (28) can be therefore rewritten as follows

$$L(u)+N(u)-f(r)=0 \tag{30}$$

By the homotopy technique, a homotopy $U(r,p):\Omega\times[0,1]\to R$ can be constructed, which satisfies

$$H(U,p)=(1-p)\left[L(U)-L(U_o)\right]+p\left[A(U)-f(r)\right]=0,\quad p\in[0,1] \tag{31}$$

Or

$$H(U,p)=L(U)-L(U_o)+pL(U_o)+p\left[N(U)-f(r)\right]=0 \tag{32}$$

In the above Eqs. (31) and (32), $p\in[0,1]$ is an embedding parameter, u_o is an initial approximation of equation of Equation (28), which satisfies the boundary conditions.

Also, from Eqs. (24) and (25), we will have

$$H(U,0)=L(U)-L(U_o)=0 \tag{33}$$

$$H(U,0)=A(U)-f(r)=0 \tag{34}$$

The changing process of *p* from zero to unity is just that of $U(r,p)$ from $u_o(r)$ to $u(r)$. This is referred to homotopy in topology. Using the embedding parameter *p* as a small parameter, the solution of Eqs. (31) and (32) can be assumed to be written as a power series in p as given in Equation (35)

$$U=U_o+pU_1+p^2U_2+... \tag{35}$$

It should be pointed out that of all the values of *p* between 0 and 1, *p=1* produces the best result. Therefore, setting $p=1$, results in the approximation solution of Equation (28)

$$u=\lim_{p\to 1}U=U_o+U_1+U_2+... \tag{36}$$

The basic idea expressed above is a combination of homotopy and perturbation method. Hence, the method is called homotopy perturbation method (HPM), which has eliminated the limitations of the traditional perturbation methods. On the other hand, this technique can have full advantages of the traditional perturbation techniques. The series Equation (36) is convergent for most cases.

4.2 Application of the homotopy perturbation method to the present problem

For ease of our analysis, Equation (18) is written as

$$\frac{d^2\theta}{dX^2}-S_h\theta^2-M_a^2\theta+M^2G(1+\gamma\theta)=0 \tag{37}$$

where

$$S_h = \frac{Ra}{(1+4Rd)},\ M^2 = \frac{Nc(1-\varepsilon)}{(1+4Rd)} + \frac{Nr}{(1+4Rd)} + \frac{H}{(1+4Rd)},\quad G = \frac{Q}{(1+4Rd)}$$

According to homotopy perturbation method (HPM), one can construct an homotopy for Equation (37) as

$$H(\theta, p) = (1-p)\left[\frac{d^2\theta}{dX^2}\right] + p\left[\frac{d^2\theta}{dX^2} - S_h\theta^2 - M^2\theta + M^2G(1+\gamma\theta)\right] \tag{38}$$

where $p \in [0,1]$ is an embedding parameter. For $p = 0$ and $p = 1$ we have

$$\theta(X,0) = \theta_0(X) \quad , \quad \theta(X,1) = \theta_0(X) \tag{39}$$

Note that when p increases from $0 to 1$, $\theta(X, p)$ varies from $\theta_0(X)$ to $\theta_0(X)$.

Supposing that the solution of Equation (18) can be expressed in a series in p:

$$\theta(X) = \theta_0(X) + p\theta_1(X) + p^2\theta_2(X) + p^3\theta_2(X) + \ldots = \sum_{i=0}^{n} p^i\theta_i(X) \tag{40}$$

When Eq. (40) is substituted into Eq. (38) and then expands, after the collection of like terms with the same order of p together, the resulting equation appears in form of polynomial in p. On equating each coefficient of the resulting polynomial in p to zero, we arrived at a set of differential equations and the corresponding boundary conditions as

$$p^0: \quad \frac{d^2\theta_0}{dX^2}(X) = 0, \quad \theta_0(0) = 1 \quad \theta_0'(1) = 0 \tag{41}$$

$$p^1: \quad \frac{d^2\theta_1}{dX^2} + M^2G\gamma\theta_0 - S_h\theta_0^2 - M^2\theta_0 + M^2G = 0, \quad \theta_1(0) = 0 \quad \theta_1'(1) = 0 \tag{42}$$

$$p^2: \quad \frac{d^2\theta_2}{dX^2} + M^2G\gamma\theta_1 - S_h\theta_0\theta_1 - M^2\theta_1 = 0, \quad \theta_2(0) = 0 \quad \theta_2'(1) = 0 \tag{43}$$

$$p^3: \quad \frac{d^2\theta_3}{dX^2} + M^2G\gamma\theta_2 - S_h\theta_1^2 - 2S_h\theta_0\theta_2 - M^2\theta_1 + M^2G = 0, \quad \theta_3(0) = 0 \quad \theta_3'(1) = 0 \tag{44}$$

$$p^4: \quad \frac{d^2\theta_4}{dX^2} - M^2\theta_3 - 2S_h\theta_1\theta_2 - 2S_h\theta_0\theta_3 + M^2G\gamma\theta_3 = 0, \quad \theta_4(0) = 0 \quad \theta_4'(1) = 0 \tag{45}$$

$$p^5: \quad \frac{d^2\theta_5}{dX^2} - S_h\theta_1\theta_3 + M^2G\gamma\theta_4 - M^2\theta_4 - S_h\theta_2^2 - 2S_h\theta_0\theta_4 = 0, \quad \theta_5(0) = 0 \quad \theta_5'(1) = 0 \tag{46}$$

$$p^6: \quad \frac{d^2\theta_6}{dX^2} + M^2G\gamma\theta_5 - 2S_h\theta_0\theta_5 - 2S_h\theta_1\theta_4 - M^2\theta_5 - 2S_h\theta_2\theta_3 = 0, \quad \theta_6(0) = 0 \quad \theta_6'(1) = 0 \tag{47}$$

$$p^7: \quad \frac{d^2\theta_7}{dX^2} + M^2G\gamma\theta_6 - 2S_h\theta_1\theta_5 - 2S_h\theta_0\theta_6 - M^2\theta_6 - 2S_h\theta_2\theta_4 = 0, \quad \theta_7(0) = 0 \quad \theta_7'(1) = 0 \tag{48}$$

$$p^8: \quad \frac{d^2\theta_8}{dX^2} + M^2G\gamma\theta_7 - 2S_h\theta_3\theta_4 - 2S_h\theta_1\theta_6 - M^2\theta_7 - 2S_h\theta_0\theta_7 - 2S_h\theta_2\theta_5 = 0, \quad \theta_8(0) = 0 \quad \theta_8'(1) = 0 \tag{49}$$

$$p^9: \quad \frac{d^2\theta_9}{dX^2} - 2S_h\theta_0\theta_8 - 2S_h\theta_2\theta_6 + M^2G\gamma\theta_8 - S_h\theta_4^2 - 2S_h\theta_3\theta_5 - 2S_h\theta_1\theta_7 - M^2\theta_8 = 0, \quad \theta_9(0) = 0 \quad \theta_9'(1) = 0 \tag{50}$$

On solving the above (Equations 41-50), we arrived at

$$\theta_0(X) = 1 \tag{51}$$

$$\theta_1(X) = \frac{\left[M^2\left[1 - G(1+\gamma)\right] + S_h\right]}{2}\left(X^2 - 1\right) \tag{52}$$

$$\theta_2(X) = \frac{\left[M^2\left[1 - G(1+\gamma)\right] + S_h\right]\left(M^2 + 2S_h - M^2G\gamma\right)}{24}\left(X^4 - 6X^2 + 5\right) \tag{53}$$

$$\theta_3(X) = \left[\begin{array}{l} \left(S_h\left(\frac{\left[M^2\left[1 - G(1+\gamma)\right] + S_h\right]}{2}\right)^2 + \right. \\ \left.\frac{\left(M^2 + 2S_h - M^2G\gamma\right)}{12}\left(\frac{\left[M^2\left[1 - G(1+\gamma)\right] + S_h\right]\left(M^2 + 2S_h - M^2G\gamma\right)}{2}\right)\right)\frac{X^6}{30} - \\ \left(2S_h\left(\frac{\left[M^2\left[1 - G(1+\gamma)\right] + S_h\right]}{2}\right)^2 + \right. \\ \left.\frac{\left(M^2 + 2S_h - M^2G\gamma\right)}{2}\left(\frac{\left[M^2\left[1 - G(1+\gamma)\right] + S_h\right]\left(M^2 + 2S_h - M^2G\gamma\right)}{2}\right)\right)\frac{X^4}{12} + \\ \left(S_h\left(\frac{\left[M^2\left[1 - G(1+\gamma)\right] + S_h\right]}{2}\right)^2 + \right. \\ \left.\frac{5\left(M^2 + 2S_h - M^2G\gamma\right)}{12}\left(\frac{\left[M^2\left[1 - G(1+\gamma)\right] + S_h\right]\left(M^2 + 2S_h - M^2G\gamma\right)}{2}\right)\right)\frac{X^2}{2} - \\ \left(\frac{11}{30}S_h\left(\frac{\left[M^2\left[1 - G(1+\gamma)\right] + S_h\right]}{2}\right)^2 + \right. \\ \left.\frac{61\left(M^2 + 2S_h - M^2G\gamma\right)}{360}\left(\frac{\left[M^2\left[1 - G(1+\gamma)\right] + S_h\right]\left(M^2 + 2S_h - M^2G\gamma\right)}{2}\right)\right) \end{array}\right] \tag{54}$$

In the same manner, the expressions for $\theta_4(X), \theta_5(X), \theta_5(X), \theta_6(X), \theta_7(X), \theta_8(X), \theta_9(X)$

, were obtained. However, they are too large expressions to be included in this paper.

From the definition, the solution of Equation (18) in HPM domain is

$$\theta(X) = \theta_0(X) + p\theta_1(X) + p^2\theta_2(X) + p^3\theta_3(X) + p^4\theta_4(X) + p^5\theta_5(X) + p^6\theta_6(X) + p^7\theta_7(X) + p^8\theta_8(X) + p^9\theta_9(X) + \ldots \quad (55)$$

It should be pointed out that of all the values of p between 0 and 1, $p=1$ produces the best result. Therefore, setting $p=1$, results in the approximation solution of Equation (55)

$$\theta(X) = \lim_{p\to 1}\theta(X) = \theta_0(X) + \theta_1(X) + \theta_2(X) + \theta_3(X) + \theta_4(X) + \theta_5(X) + \theta_6(X) + \theta_7(X) + \theta_8(X) + \theta_9(X) + \ldots \quad (56)$$

On substituting Equation (51-54), one arrives at

$$\theta(X) = 1 - \frac{\left[M^2\left[1-G(1+\gamma)\right]+S_h\right]}{2}\left(1-X^2\right) + \frac{\left[M^2\left[1-G(1+\gamma)\right]+S_h\right]\left(M^2+2S_h-M^2G\gamma\right)}{24}\left(X^4-6X^2+5\right) + \left[\begin{array}{l} \left(S_h\left(\frac{\left[M^2\left[1-G(1+\gamma)\right]+S_h\right]}{2}\right)^2 + \frac{\left(M^2+2S_h-M^2G\gamma\right)}{12}\left(\frac{\left[M^2\left[1-G(1+\gamma)\right]+S_h\right]\left(M^2+2S_h-M^2G\gamma\right)}{2}\right)\right)\frac{X^6}{30} - \\ \left(2S_h\left(\frac{\left[M^2\left[1-G(1+\gamma)\right]+S_h\right]}{2}\right)^2 + \frac{\left(M^2+2S_h-M^2G\gamma\right)}{2}\left(\frac{\left[M^2\left[1-G(1+\gamma)\right]+S_h\right]\left(M^2+2S_h-M^2G\gamma\right)}{2}\right)\right)\frac{X^4}{12} + \\ \left(S_h\left(\frac{\left[M^2\left[1-G(1+\gamma)\right]+S_h\right]}{2}\right)^2 + \frac{5\left(M^2+2S_h-M^2G\gamma\right)}{12}\left(\frac{\left[M^2\left[1-G(1+\gamma)\right]+S_h\right]\left(M^2+2S_h-M^2G\gamma\right)}{2}\right)\right)\frac{X^2}{2} - \\ \left(\frac{11}{30}S_h\left(\frac{\left[M^2\left[1-G(1+\gamma)\right]+S_h\right]}{2}\right)^2 + \frac{61\left(M^2+2S_h-M^2G\gamma\right)}{360}\left(\frac{\left[M^2\left[1-G(1+\gamma)\right]+S_h\right]\left(M^2+2S_h-M^2G\gamma\right)}{2}\right)\right) \end{array}\right] + \ldots \quad (57)$$

where

$$S_h = \frac{Ra}{(1+4Rd)}, \qquad M^2 = \frac{Nc(1-\varepsilon)}{(1+4Rd)} + \frac{Nr}{(1+4Rd)} + \frac{H}{(1+4Rd)}, \qquad G = \frac{Q}{(1+4Rd)}$$

5. Exact analytical solution for model validation

For the purpose of validation of the model results, we developed exact analytical solution for a porous fin with constant thermal conductivity. The dimensionless governing differential equation is given as

$$\frac{d^2\theta}{dX^2} - \frac{Ra}{(1+4Rd)}\theta^2 - \frac{\left(Nc(1-\varepsilon)+Nr+H\right)}{(1+4Rd)}\theta = 0 \tag{58}$$

In order to find exact analytical solution for Equation (58), taking the transformation $\frac{d\theta}{dX} = \phi$, we arrived at

$$\phi\frac{d\phi}{dX} - \frac{Ra}{(1+4Rd)}\theta^2 - \frac{\left(Nc(1-\varepsilon)+Nr+H\right)}{(1+4Rd)}\theta = 0 \tag{59}$$

On integrating Equation (59) wrt θ, we have

$$\frac{\phi^2}{2} - \frac{Ra}{3(1+4Rd)}\theta^3 - \frac{\left(Nc(1-\varepsilon)+Nr+H\right)}{(1+4Rd)}\theta^2 = C \tag{60}$$

Recall that $\phi = \frac{d\theta}{dX} \quad \rightarrow \phi^2 = \left(\frac{d\theta}{dX}\right)^2$

Therefore, Equation (60) becomes

$$\frac{1}{2}\left(\frac{d\theta}{dX}\right)^2 - \frac{Ra}{3(1+4Rd)}\theta^3 - \frac{\left(Nc(1-\varepsilon)+Nr+H\right)}{(1+4Rd)}\theta^2 = C \tag{61}$$

With the application of the first boundary condition, $X = 1, \quad \frac{d\theta}{dX} = 0 \quad \rightarrow X = 1, \quad \theta = \theta_o$

$$C = -\frac{Ra}{3(1+4Rd)}\theta_o^3 - \frac{\left(Nc(1-\varepsilon)+Nr+H\right)}{(1+4Rd)}\theta_o^2 \tag{62}$$

On substituting Equation (62) into Equation (61), we arrived at

$$\frac{1}{2}\left(\frac{d\theta}{dX}\right)^2 - \frac{Ra}{3(1+4Rd)}\left(\theta^3-\theta_o^3\right) - \frac{\left(Nc(1-\varepsilon)+Nr+H\right)}{(1+4Rd)}\left(\theta^2-\theta_o^2\right) = 0 \tag{63}$$

Which could be written as

$$\left(\frac{d\theta}{dX}\right)^2 - \frac{2Ra}{3(1+4Rd)}\theta^3 - \frac{\left(Nc(1-\varepsilon)+Nr+H\right)}{(1+4Rd)}\theta^2 + \frac{2Ra}{3(1+4Rd)}\theta_o^3 + \frac{\left(Nc(1-\varepsilon)+Nr+H\right)}{(1+4Rd)}\theta_o^2 = 0 \qquad (64)$$

Then

$$dX = \frac{-d\theta}{\sqrt{\frac{2Ra}{3(1+4Rd)}\theta^3 + \frac{\left(Nc(1-\varepsilon)+Nr+H\right)}{(1+4Rd)}\theta^2 - \frac{2Ra}{3(1+4Rd)}\theta_o^3 - \frac{\left(Nc(1-\varepsilon)+Nr+H\right)}{(1+4Rd)}\theta_o^2}} \qquad (65)$$

Since θ decreases as x increases, the negative sign is used in when taking the square root .

Integrating Equation (65)

$$\int_0^X dX = -\int_{\theta_o}^{\theta} \frac{d\theta}{\sqrt{\frac{2Ra}{3(1+4Rd)}\theta^3 + \frac{\left(Nc(1-\varepsilon)+Nr+H\right)}{(1+4Rd)}\theta^2 - \frac{2Ra}{3(1+4Rd)}\theta_o^3 - \frac{\left(Nc(1-\varepsilon)+Nr+H\right)}{(1+4Rd)}\theta_o^2}} \qquad (66)$$

which gives

$$X = \int_{\theta}^{\theta_o} \frac{d\theta}{\sqrt{\frac{2Ra}{3(1+4Rd)}\theta^3 + \frac{\left(Nc(1-\varepsilon)+Nr+H\right)}{(1+4Rd)}\theta^2 - \frac{2Ra}{3(1+4Rd)}\theta_o^3 - \frac{\left(Nc(1-\varepsilon)+Nr+H\right)}{(1+4Rd)}\theta_o^2}} \qquad (67)$$

Suppose that

$$G(\theta; Ra, M, \theta_o) = \int_{\theta}^{\theta_o} \frac{d\theta}{\sqrt{\frac{2Ra}{3(1+4Rd)}\theta^3 + \frac{\left(Nc(1-\varepsilon)+Nr+H\right)}{(1+4Rd)}\theta^2 - \frac{2Ra}{3(1+4Rd)}\theta_o^3 - \frac{\left(Nc(1-\varepsilon)+Nr+H\right)}{(1+4Rd)}\theta_o^2}} \qquad (68)$$

where

$$M = Nc(1-\varepsilon) + Nr + H$$

For instant

$$G(\theta;1,1,\theta_o) = \sqrt{\frac{\alpha_1^2}{3+6\theta_o+\alpha_1}} \left\{ \frac{\left[\begin{array}{l} \sqrt{\frac{3+6\theta_o+\alpha_1}{\alpha_1}}\sqrt{\frac{-3-6\theta_o+\alpha_1}{\alpha_1}}\,EllipticF\left(\sqrt{\frac{3+6\theta_o+\alpha_1}{2\alpha_1}}, \sqrt{\frac{2\alpha_1}{3+6\theta_o+\alpha_1}}\right)\alpha_2 \\ -3\sqrt{\frac{3+2\theta_o+\alpha_1+4\theta}{\alpha_1}}\sqrt{\theta_o-\theta}\sqrt{\frac{-3-2\theta_o+\alpha_1+4\theta}{\alpha_1}}\,EllipticF\left(\sqrt{\frac{3+2\theta_o+\alpha_1+4\theta}{2\alpha_1}}, \sqrt{\frac{2\alpha_1}{3+6\theta_o+\alpha_1}}\right)\alpha_3 \end{array} \right]}{\alpha_2\alpha_3} \right\} \qquad (69)$$

Where

$$\alpha_1 = \sqrt{57 - 12\theta_o - 12\theta_o^2}$$

$$\alpha_2 = \sqrt{6\theta^3 - 18\theta + 9\theta^2 - 6\theta_o^3 + 18\theta_o - 9\theta_o^2}$$

$$\alpha_3 = \sqrt{2 - 2\theta_o - 2\theta_o^2}$$

Therefore, the exact solution of Equation (60) in implicit form is given by

$$X = G\left(\theta; Ra, M, \theta_o\right) \tag{70}$$

Where the unknown θ_o in the solution can be determined from the second boundary condition

$$X = 0, \quad \theta = 1 \quad \rightarrow 1 = G\left(0; Ra, M, \theta_o\right) \quad \rightarrow G\left(0; Ra, M, \theta_o\right) = 1$$

i.e. for any given S_h,, and Q, θ_o is obtained from

$$G\left(0; Ra, M, \theta_o\right) = 1 \tag{71}$$

And EllipticF in Equation (69) is the incomplete elliptic integral of the first kind defined as

$$EllipticF\left(X, K\right) = \int_0^X \frac{d\tau}{\sqrt{1-\tau^2}\sqrt{1-K^2\tau^2}} \tag{72a}$$

This function can be exactly and analytically evaluated as follows

Let $\tau = sin\vartheta, \quad x = sin\phi$

$$EllipticF\left(\phi, K\right) = \int_0^\phi \frac{d\vartheta}{\sqrt{1-K^2 sin\vartheta}} \tag{72b}$$

In order to evaluate the integral, we expand the integral in the form

$$\frac{1}{\sqrt{1-K^2 sin^2\vartheta}} = 1 + \frac{K^2}{2} sin^2\vartheta + \frac{3K^4}{8} sin^4\vartheta + \frac{5K^6}{16} sin^6\vartheta + \frac{35K^8}{128} sin^8\vartheta + ... \tag{73}$$

which could written as

$$\frac{1}{\sqrt{1-K^2 sin^2\vartheta}} - 1 = \frac{K^2}{2} sin^2\vartheta + \frac{3K^4}{8} sin^4\vartheta + \frac{5K^6}{16} sin^6\vartheta + \frac{35K^8}{128} sin^8\vartheta + ... + \left(\prod_{n=1}^{N} \frac{2n-1}{2n}\right) K^{2n} sin^{2n}\vartheta \tag{74}$$

Generally, we can write

$$\frac{1}{\sqrt{1-K^2 sin^2 \vartheta}} = 1 + \sum_{n=1}^{N} \left(\prod_{n=1}^{N} \frac{2n-1}{2n} \right) K^{2n} sin^{2n} \vartheta \tag{75}$$

The above series is uniformly convergent for all ϑ, and may, therefore, be integrated term by term. Then, we have

$$EllipticF(\phi, K) = \int_0^{\phi} \left\{ 1 + \sum_{n=1}^{N} \left(\prod_{n=1}^{N} \frac{2n-1}{2n} \right) K^{2n} sin^{2n} \vartheta \right\} d\vartheta \tag{76}$$

But

$$\int sin^{2n} \vartheta d\vartheta = \frac{-cos\vartheta}{2n} \left\{ sin^{2n-1} \vartheta + \sum_{k=1}^{n-1} \frac{(2n-1)(2n-3)...(2n-2k+1)}{2^k (n-1)(n-2)...(n-k)} sin^{2n-2k-1} \vartheta \right\} + \frac{(2n-1)!!}{2^n n!} \vartheta \tag{77}$$

Therefore

$$EllipticF(\phi, K) = \left\{ \phi + \sum_{n=1}^{N} \left(\prod_{n=1}^{N} \frac{2n-1}{2n} \right) K^{2n} \left\{ \begin{array}{l} \frac{-cos\phi}{2n} \left\{ sin^{2n-1} \phi + \sum_{k=1}^{n-1} \frac{(2n-1)(2n-3)...(2n-2k+1)}{2^k (n-1)(n-2)...(n-k)} sin^{2n-2k-1} \phi \right\} \\ + \frac{(2n-1)!!}{2^n n!} \phi \end{array} \right\} \right\} \tag{78}$$

The symbolic and numerical calculations involved in the function $G(0; Rd, Ra, M, \theta_o)$ were carried out via Wolfram's Mathematica.

4. Results and Discussion

The results of the approximate analytical methods of solution for the non-linear thermal model as developed in this work are verified by the numerical method (NM) and the Exact analytical method. The results of the differential transformation method (DTM) and homotopy perturbation method (HPM) agrees very well with the results of the numerical method as shown in Tables 1 and 2. Also, the Tables show that the results of DTM and HPM are highly accurate and agree very well with the numerical method.

Table 1: Comparison of results *for Rd = 0.5, ε = 0.1, Ra = 0.4, Nc = 0.3, Q=0, Nr = 0.2, H = 0.1*

X	DTM	NUM	| NM-DTM |
0.00	0.863499158	0.863499231	0.000000073
0.05	0.863828540	0.863828568	0.000000028
0.10	0.864817031	0.864817090	0.000000059
0.15	0.866465671	0.866465743	0.000000072
0.20	0.868776195	0.868776261	0.000000066
0.25	0.871751037	0.871751104	0.000000067
0.30	0.875393336	0.875393404	0.000000068
0.35	0.879706946	0.879707010	0.000000064
0.40	0.884696438	0.884696500	0.000000062
0.45	0.890367120	0.890367181	0.000000061
0.50	0.896725040	0.896725096	0.000000056
0.55	0.903777007	0.903777060	0.000000053
0.60	0.911530606	0.911530658	0.000000052
0.65	0.919994212	0.919994259	0.000000047
0.70	0.929177015	0.929177056	0.000000041
0.75	0.939089039	0.939089079	0.000000040
0.80	0.949741166	0.949741203	0.000000037
0.85	0.961145166	0.961145189	0.000000023
0.90	0.973313722	0.973313764	0.000000042
0.95	0.986260463	0.986260549	0.000000086
1.00	1.000000000	1.000000000	0.000000000

Table 2: Comparison of results *of NM and HPM for θ(X) for Rd = 0.5, ε = 0.1, Ra = 0.4, Nc = 0.3, Q=0, Nr = 0.2, H = 0.1*

X	NM	HPM	NM – DTM |
0.00	0.863499231	0.863499664	0.000000433
0.05	0.863828568	0.863829046	0.000000478
0.10	0.864817090	0.864817539	0.000000449
0.15	0.866466182	0.866465743	0.000000439
0.20	0.868776709	0.868776261	0.000000448
0.25	0.871751555	0.871751104	0.000000451
0.30	0.875393859	0.875393404	0.000000455
0.35	0.879707472	0.879707010	0.000000462
0.40	0.884696967	0.884696500	0.000000467
0.45	0.890367650	0.890367181	0.000000469
0.50	0.896725569	0.896725096	0.000000473
0.55	0.903777531	0.903777060	0.000000471
0.60	0.911531120	0.911530658	0.000000462
0.65	0.919994710	0.919994259	0.000000451
0.70	0.929177488	0.929177056	0.000000432
0.75	0.939089476	0.939089079	0.000000397
0.80	0.949741555	0.949741203	0.000000352
0.85	0.961145491	0.961145189	0.000000302
0.90	0.973313964	0.973313764	0.000000200
0.95	0.986260599	0.986260549	0.000000005
1.00	1.000.000.000	1.000.000.000	0.000000000

Figure 2 shows the effects of porous parameter or porosity on the temperature distribution in the porous fin are shown. From the figures, as the porosity parameter increases, the temperature decreases rapidly and the rate of heat transfer (the convective-radiative heat transfer) through the fin increases as the temperature in the fin drops faster (becomes steeper reflecting high base heat flow rates) as depicted in the figures. The rapid decrease in fin temperature due to increase in the porosity parameter is because as porosity parameter, Raleigh number increases, the permeability of the porous fin increases and therefore the ability of the working fluid to penetrate through the fin pores increases, the effect of buoyancy force increases and thus the fin convects more heat, the rate of heat transfer from the fin is enhanced and the thermal performance of the fin is increased. Therefore, increase in the porosity of the fin improves fin efficiency due to increasing in convection heat transfer.

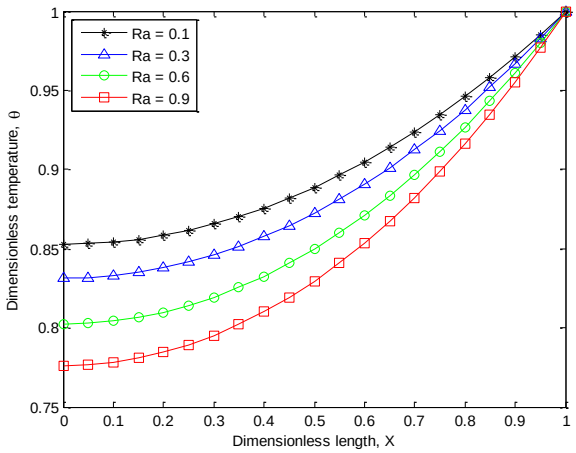

Figure 2 Dimensionless temperature distribution in the fin parameters for varying porous parameter when Rd = 0.5, Nc = 0.6, Nr = 0.1, ε = 0.8 and Ha =0.7, Q =0

Figure 3 show the effects of conduction-convection parameter on the temperature distribution in the fin. The figure depicts that as the conduction-convection parameter increases, the rate of heat transfer through the fin increases as the temperature in the fin drops faster (becomes steeper reflecting high base heat flow rates) as depicted in the figures. The profile has steepest temperature gradient at lower value of the conduction-convection term, but its much higher value gotten from the lower value of thermal conductivity than the other values of *Nc* in the profiles produces a lower heat-transfer rate. This shows that the thermal performance or efficiency of the fin is favoured at low values of convective parameter since the aim (high effective use of the fin) is to minimize the temperature decrease along the fin length, where the best possible scenario is when $T=T_b$ everywhere. It must be pointed out that a small value of M correspond to a relatively short and thick fins of poor thermal conductivity and high value of M implies a long fin or fin with low value of thermal conductivity. Since, the thermal performance or efficiency of the fin is favoured at low values of convective fin parameter, very long fins are to be avoided in practice.

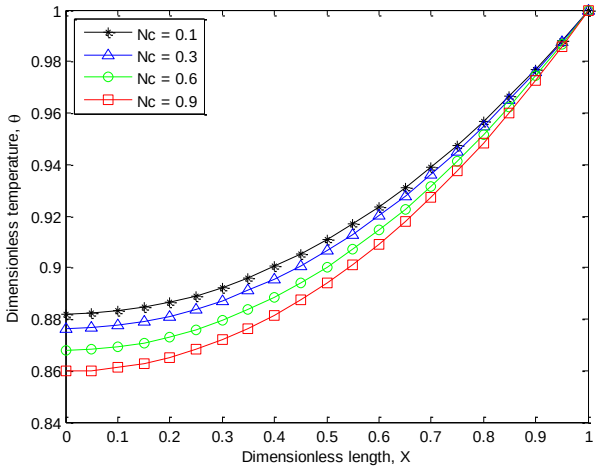

Figure 3 Dimensionless temperature distribution in the fin parameters for varying convection-conduction parameter when Rd = 0.5, Ra = 0.3, Nr = 0.2, ε = 0.7, Q=0 and Ha =0.6.

The effects of conduction-radiation parameter are shown in Figure 4. The Figure shows that increase in the conduction-radiation parameter, the rate of heat transfer through the fin increases.

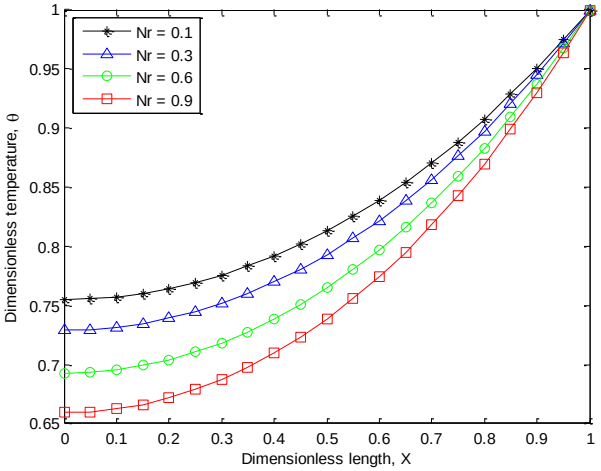

Figure 4 Dimensionless temperature distribution in the fin parameters for varying radiation-conduction parameter when Rd = 0.8, Ra = 0.7, Nc = 0.5, ε = 0.2, Q=0 and Ha =0.3.

Figure 5 shows that effects of magnetic parameter, Hartman number on the temperature distribution in the porous fin. The figure depicts that the induced magnetic field in the fin can improve heat transfer through porous fins. This fact is also depicted in Figure 6 and it is also shown that conduction-radiation parameter increases the thermal performance of the fin. From 2-6, it is shown that increase in porosity, convective, radiative and magnetic parameters increase the rate of heat transfer from the fin and consequently improve the efficiency of the fin.

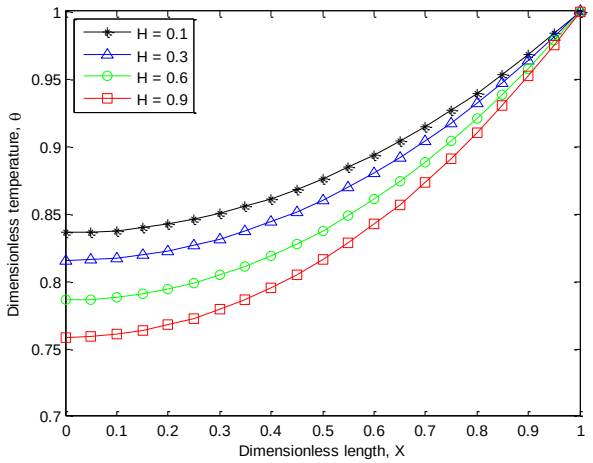

Figure 5 Dimensionless temperature distribution in the fin parameters for varying Hartman number (magnetic parameter), when Rd = 0.6, Ra = 0.5, Nc = 0.1, Q=0, Nr = 0.7 and ε = 0.4.

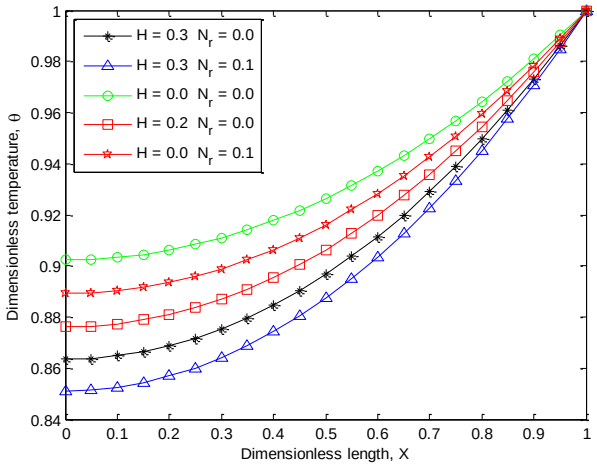

Figure 6 Dimensionless temperature distribution in the fin parameters for varying Hartman parameters and surface-ambient radiation parameters, when Rd = 0.5, Ra = 0.4, Nc = 0.3, Q=0 and ε = 0.1.

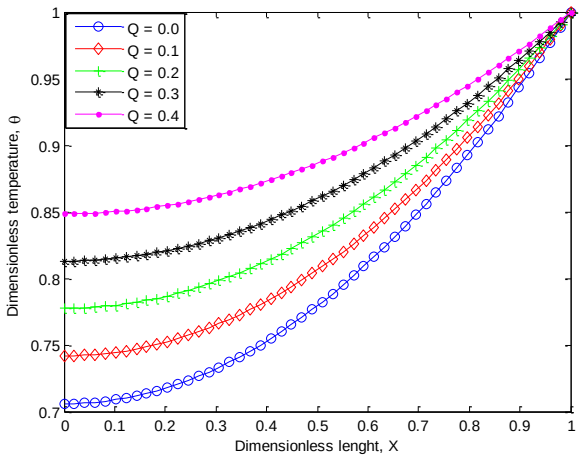

Figure 7 Dimensionless temperature distribution in the fin parameters for varying internal heat generation parameters, when Rd = 0.25, Ra = 2.0,
Nc = 1.0, Nr=0.8, γ=0.2, H=0.4 and ε = 0.2.

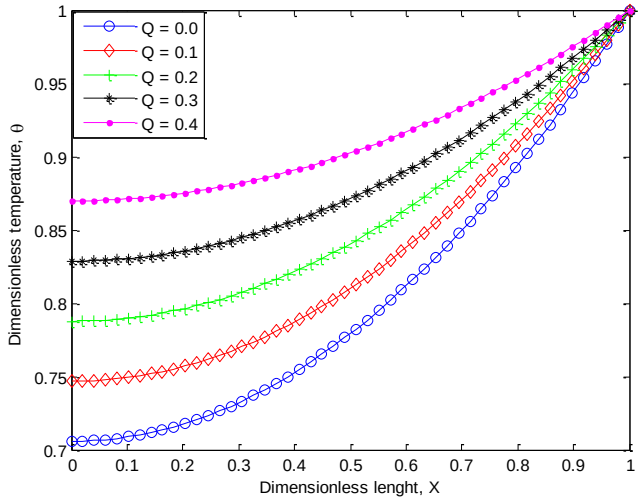

Figure 8 Dimensionless temperature distribution in the fin parameters for varying internal heat generation parameters, when Rd = 0.25, Ra = 2.0, Nc = 1.0, Nr=0.8, γ=0.4, H=0.4 and ε = 0.2.

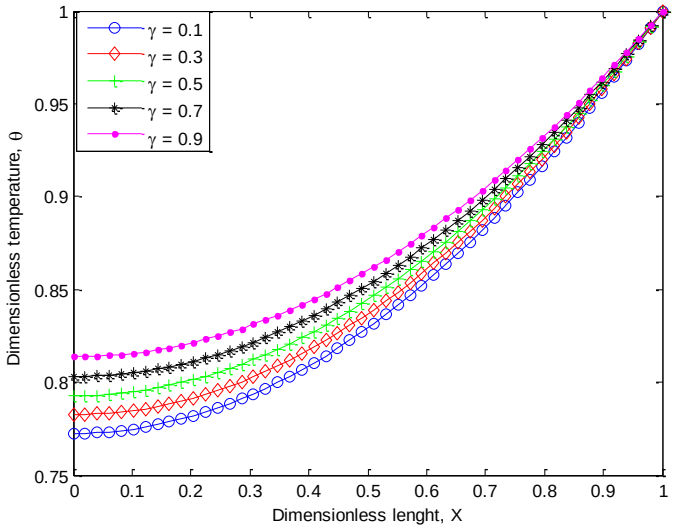

Fig. 9 Dimensionless temperature distribution in the fin parameters for varying temperature-dependent internal heat generation parameters, when Rd = 0.25, Ra = 2.0, Nr=0.8, Nc = 1.0, H=0.4, Q=0.2 and ε = 0.2.

Figures 7 and 8 show the effects of internal heat generation parameter on the temperature distribution in the porous fin while Figures 9 and 10 depict the effects of temperature-dependent internal heat generation parameter on the temperature distribution in the fin. From the figures, as the internal heat generation parameters increase, the temperature gradient of the fins decreases and consequently, the rate of heat transfer in the fin decreases. It should be stated that fins with porous material give superior performance with a significant reduction in weight compared with solid metal fins because of its low thermal conductivity and large area of the material when it comes in contact with the cooling fluid.

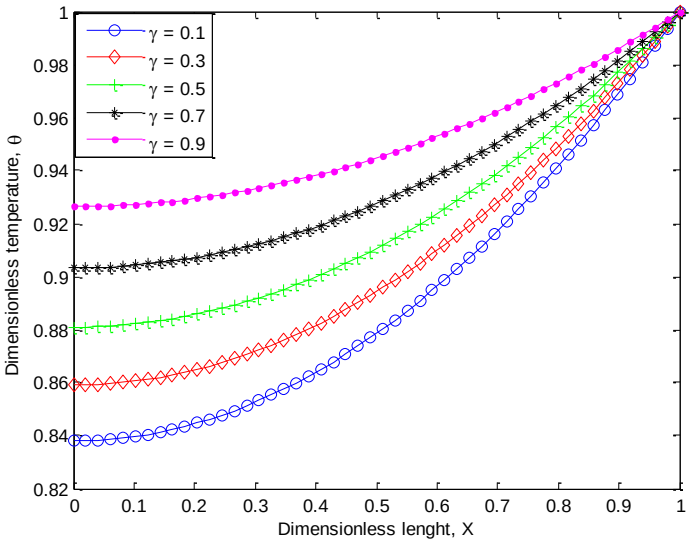

Figure 10 Dimensionless temperature distribution in the fin parameters for varying temperature-dependent internal heat generation parameters, when Rd = 0.25, Ra = 2.0, Nr=0.8, Nc = 1.0, H=0.4, Q=0.4 and ε = 0.2.

Figure 11 present the comparison of the results of the Exact analytical, differential transformation, homotopy perturbation methods. Again, it is shown that the results of the differential transformation method and homotopy perturbation method agrees very well with the results of the exact analytical method. The attest to the high accuracy of the DTM and HPM.

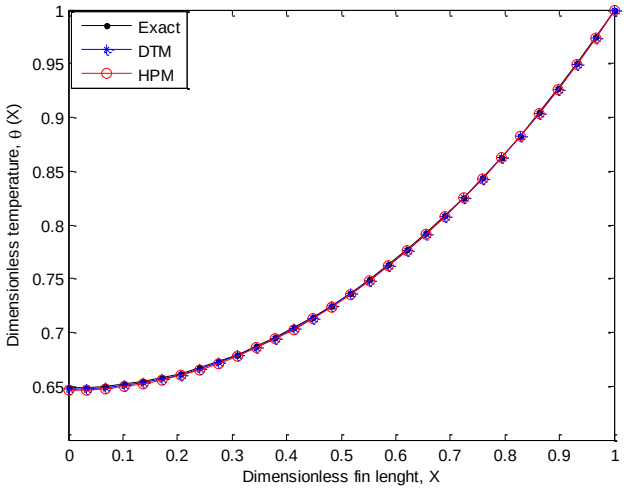

Figure 11 Comparison of the results of the Exact analytical, differential transformation, homotopy perturbation methods.

6. Conclusion

In this work, homotopy perturbation and differential transform methods have been used for comparative analysis of thermal behaviour of convective-radiative porous fin subjected to magnetic field. The results of the approximate analytical method are verified by the numerical method. The results of the differential transformation method and homotopy perturbation method agree very well with the results of the numerical method. Also, parametric study revealed that increase in magnetic field, porosity, convective, radiative and parameters increase the rate of heat transfer from the fin and consequently improve the efficiency of the fin.

References

Amirkolaei, S. R., Ganji, D. D., & Salarian, H. (2014). Determination of temperature distribution for porous fin which is exposed to uniform magnetic field to a vertical isothermal surface by homotopy analysis method and collocation method. *Indian J. Sci. Res*, *1*(2), 215-222.

Bhanja, D., & Kundu, B. (2011). Thermal analysis of a constructal T-shaped porous fin with radiation effects. *International journal of refrigeration*, *34*(6), 1483-1496.

Darvishi, M. T., Gorla, R. S. R., Khani, F., & Aziz, A. (2015). Thermal performance of a porus radial fin with natural convection and radiative heat losses. *Thermal Science*, *19*(2), 669-678.

Ghasemi, S. E., Valipour, P., Hatami, M., & Ganji, D. D. (2014). Heat transfer study on solid and porous convective fins with temperature-dependent heat generation using efficient analytical method. *Journal of Central South University*, *21*(12), 4592-4598.

Gorla, R. S., Darvishi, M. T., & Khani, F. (2013). Effect of variable thermal conductivity on natural convection and radiation in porous. *Thermal Energy Power Eng*, *2*, 79-85.

Gorla, Rama & Bakier, A.Y. (2007). Thermal analysis of natural convection and radiation in porous fins. International Communications in Heat and Mass Transfer. 38. 638-645. 10.1016/j.icheatmasstransfer.2010.12.024.

Hatami, M., & Ganji, D. D. (2013). Thermal performance of circular convective–radiative porous fins with different section shapes and materials. *Energy Conversion and Management*, *76*, 185-193.

Hatami, M., & Ganji, D. D. (2014a). Investigation of refrigeration efficiency for fully wet circular porous fins with variable sections by combined heat and mass transfer analysis. *International journal of refrigeration*, *40*, 140-151.

Hatami, M., & Ganji, D. D. (2014b). Thermal behavior of longitudinal convective–radiative porous fins with different section shapes and ceramic materials (SiC and Si3N4). *Ceramics International*, *40*(5), 6765-6775.

Hatami, M., Ahangar, G. R. M., Ganji, D. D., & Boubaker, K. (2014). Refrigeration efficiency analysis for fully wet semi-spherical porous fins. *Energy conversion and management*, *84*, 533-540.

Hatami, M., Hasanpour, A., & Ganji, D. D. (2013). Heat transfer study through porous fins (Si3N4 and AL) with temperature-dependent heat generation. *Energy Conversion and Management*, *74*, 9-16.

Hoshyar HA, Ganji DD, Abbasi M (2015). Determination of Temperature Distribution for Porous Fin with Temperature-Dependent Heat Generation by Homotopy Analysis Method. J Appl Mech Eng 4: 153. doi:10.4172/2168- 9873.1000153

Hoshyar, H. A., Ganji, D. D., & Majidian, A. R. (2016). Least square method for porous fin in the presence of uniform magnetic field. *Journal of applied fluid mechanics*, *9*(2), 661-668.

Hoshyar, H. A., Rahimipetroudi, I., Ganji, D. D., & Majidian, A. R. (2015). Thermal performance of porous fins with temperature-dependent heat generation via the homotopy perturbation method and collocation method. *Journal of Applied Mathematics and Computational Mechanics*, *14*(4), 53-65.

Kiwan, S., and Al-Nimr, M. A. (July 14, 2000). Using Porous Fins for Heat Transfer Enhancement. ASME. *J. Heat Transfer*. August 2001; 123(4): 790–795. https://doi.org/10.1115/1.1371922

Kiwan, Suhil & Zeitoun, Obida. (2008). Natural convection in a horizontal cylindrical annulus using porous fins. International Journal of Numerical Methods for Heat & Fluid Flow. 18. 618-634. 10.1108/09615530810879747.

Kiwan, Suhil. (2007a). Effect of radiative losses on the heat transfer from porous fins. International Journal of Thermal Sciences. 46. 1046-1055. 10.1016/j.ijthermalsci.2006.11.013

Kiwan, Suhil. (2007b). Thermal Analysis of Natural Convection Porous Fins. *Transp Porous Med* **67**, 17–29 https://doi.org/10.1007/s11242-006-0010-3

Kundu, B. (2007). Performance and optimization analysis of SRC profile fins subject to simultaneous heat and mass transfer. *International journal of heat and mass transfer*, *50*(7-8), 1545-1558.

Kundu, Balaram & Bhanja, Dipankar & Lee, Kwan-Soo. (2012). A model on the basis of analytics for computing maximum heat transfer in porous fins. International Journal of Heat and Mass Transfer. 55. 10.1016/j.ijheatmasstransfer.2012.07.069.

Kundu, Balaram & Bhanja, Dipankar. (2011). An analytical prediction for performance and optimum design analysis of porous fins. International Journal of Refrigeration. 34. 337-352. 10.1016/j.ijrefrig.2010.06.011.

Moradi, A., Hayat, T., & Alsaedi, A. (2014). Convection-radiation thermal analysis of triangular porous fins with temperature-dependent thermal conductivity by DTM. *Energy Conversion and Management*, *77*, 70-77.

Petroudi, R. I., Ganji, D. D., Shotorban, B. A., Nejad, K. M., Rahimi, E., Rohollahtabar, R., & Taherinia, F. (2012). Semi-analytical method for solving non-linear equation arising of natural convection porous fin. *Thermal Science*, *16*(5), 1303-1308.

Rostamiyan, Y., Ganji, D. D., Petroudi, R. I., & Nejad, K. M. (2014). Analytical investigation of nonlinear model arising in heat transfer through the porous fin. *Thermal science*, *18*(2), 409-417.

Saedodin, S., & Olank, M. (2011). Temperature distribution in porous fins in natural convection condition. *Journal of American Science*, *7*(6), 476-481.

Saedodin, S., & Sadeghi, S. (2013). Temperature distribution in long porous fins in natural convection condition. *Middle-East Journal of Scientific Research*, *13*(6), 812-7.

Saedodin, S., & Shahbabaei, M. (2013). Thermal analysis of natural convection in porous fins with homotopy perturbation method (HPM). *Arabian Journal for Science and Engineering*, *38*(8), 2227-2231.

Taklifi, A., Aghanajafi, C. & Akrami, H. (2010). The Effect of MHD on a Porous Fin Attached to a Vertical Isothermal Surface. *Transp Porous Med* **85**, 215–231. https://doi.org/10.1007/s11242-010-9556-1